NAVAL POSTGRADUATE SCHOOL

MONTEREY, CALIFORNIA

THESIS

AN EXPERIMENTAL APPROACH FOR STUDYING THE CREEP BEHAVIOR OF THIN FILM / SUBSTRATE INTERFACES

by

Carl L. Parks

September 2004

Thesis Advisor: Indranath Dutta

Approved for public release; distribution is unlimited

THIS PAGE INTENTIONALLY LEFT BLANK

REPORT DOCUMENTATION PAGE			Form Approved OMB No. 0704-0188
Public reporting burden for this collection of information is estimated to average 1 hour per response, including the time for reviewing instruction, searching existing data sources, gathering and maintaining the data needed, and completing and reviewing the collection of information. Send comments regarding this burden estimate or any other aspect of this collection of information, including suggestions for reducing this burden, to Washington headquarters Services, Directorate for Information Operations and Reports, 1215 Jefferson Davis Highway, Suite 1204, Arlington, VA 22202-4302, and to the Office of Management and Budget, Paperwork Reduction Project (0704-0188) Washington DC 20503.			
1. AGENCY USE ONLY ***(Leave blank)***	**2. REPORT DATE** September 2004	**3. REPORT TYPE AND DATES COVERED** Master's Thesis	
4. TITLE AND SUBTITLE: An Experimental Approach for Studying the Creep Behavior of Thin Film/Substrate Interfaces			**5. FUNDING NUMBERS**
6. AUTHOR(S) Carl L. Parks			
7. PERFORMING ORGANIZATION NAME(S) AND ADDRESS(ES) Naval Postgraduate School Monterey, CA 93943-5000			**8. PERFORMING ORGANIZATION REPORT NUMBER**
9. SPONSORING /MONITORING AGENCY NAME(S) AND ADDRESS(ES) N/A			**10. SPONSORING/MONITORING AGENCY REPORT NUMBER**
11. SUPPLEMENTARY NOTES The views expressed in this thesis are those of the author and do not reflect the official policy or position of the Department of Defense or the U.S. Government.			
12a. DISTRIBUTION / AVAILABILITY STATEMENT Approved for public release; distribution is unlimited			**12b. DISTRIBUTION CODE**

13. ABSTRACT (maximum 200 words)

Large shear stresses often develop at the interface between dissimilar materials in microelectronic devices, when they are subjected to thermo-mechanical excursions. These stresses can facilitate diffusionally accommodated interfacial sliding, or creep. A driving factor for these stresses is the thermal expansion mismatch between the adjoining materials. For narrow thin film lines, these stresses may exist over a large fraction of the film-substrate interface. This thesis explores methodologies to measure the kinetics of interfacial creep at model Al thin film/silicon substrate interfaces. A method of sample production, which involved diffusion bonding a polished Si substrate to the surface of a thin Al film deposited on a second Si substrate was developed (Si/Al/Si sandwich). When loaded edge-wise in compression, the Al thin film - Si interface are loaded in shear.

By measuring the relative displacements between the two Si substrates, the interfacial displacement rates at varying temperatures and stresses were experimentally determined. In accordance with previous results, the kinetics was given by a diffusional creep law with a threshold stress, and an activation energy representing interfacial diffusion. The activation energy was found to be unusually low, and further experimental and modeling studies are needed to better understand its origin

14. SUBJECT TERMS Interfacial Sliding, Diffusional sliding, Interfacial Creep, TMAH, PVD Al thin film, Diffusion Bonding			**15. NUMBER OF PAGES** 59
			16. PRICE CODE
17. SECURITY CLASSIFICATION OF REPORT Unclassified	**18. SECURITY CLASSIFICATION OF THIS PAGE** Unclassified	**19. SECURITY CLASSIFICATION OF ABSTRACT** Unclassified	**20. LIMITATION OF ABSTRACT** UL

NSN 7540-01-280-5500 Standard Form 298 (Rev. 2-89)
Prescribed by ANSI Std. 239-18

THIS PAGE INTENTIONALLY LEFT BLANK

Approved for public release; distribution is unlimited

AN EXPERIMENTAL APPROACH FOR STUDYING THE CREEP BEHAVIOR OF THIN FILM / SUBSTRATE INTERFACES

Carl Livingston Parks
Lieutenant Commander, United States Navy
Bachelor of Science, United States Naval Academy, 1995

Submitted in partial fulfillment of the
requirement for the degree of

MASTER OF SCIENCE IN MECHANICAL ENGINEERING

from the

NAVAL POSTGRADUATE SCHOOL
September 2004

Author: Carl Livingston Parks

Approved by: Indranath Dutta,
Thesis Advisor

Anthony J. Healy
Chairman, Department of Mechanical and Astronautical Engineering

THIS PAGE INTENTIONALLY LEFT BLANK

ABSTRACT

Large shear stresses often develop at the interface between dissimilar materials in microelectronic devices, when they are subjected to thermo-mechanical excursions. These stresses, which typically occur due to thermal expansion mismatch between the adjoining materials, are usually confined near the edges of films. However, for narrow thin film lines, these stresses may exist over a large fraction of the film-substrate interface. When the substrate is subjected to relatively high homologous temperatures, the imposed interfacial shear stress can facilitate diffusionally accommodated interfacial sliding, or interfacial creep. This thesis explores methodologies to measure the kinetics of interfacial creep at model Al thin film/silicon substrate interfaces. A method of sample production which involved diffusion bonding a polished Si substrate to the surface of a thin Al film deposited on a second Si substrate was developed. The resultant sample geometry comprises a Si/Al/Si sandwich, which when loaded edge-wise in compression, allows the Al thin film-Si interfaces to be loaded in shear.

By measuring the relative displacements between the two Si substrates, the interfacial displacement rates at varying temperatures and stresses were experimentally determined. In accordance with previous results, the kinetics was given by a diffusional creep law with a threshold stress, and an activation energy representing interfacial diffusion. The activation energy was found to be unusually low, and further experimental and modeling studies are needed to better understand its origin.

THIS PAGE INTENTIONALLY LEFT BLANK

TABLE OF CONTENTS

I. INTRODUCTION 1

II. BACKGROUND 3
- A. EXAMPLES OF INTERFACIAL SLIDING 3
  - 1. Microelectronics 3
  - 2. Metal-Matrix Composites 5
- B. POSSIBLE MECHANISMS OF INTERFACIAL SLIDING 7
- C. DIRECT MEASURMENT OF INTERFACIAL CREEP KINETICS 8

III. OBJECTIVE 11

IV. PROCESSING AND CHARACTERIZATION OF DIFFUSION BONDED Al-Si INTERFACES 13
- A. EXPERIMENTAL PROCEDURE 13
  - 1. Materials 13
  - 2. Sample Preparation 13
    - *a. Sectioning, Polishing, and Cleaning 13*
    - *b. Vacuum Evaporation of Aluminum 14*
  - 3. Diffusion Bonding 17
  - 4. Mechanical Design for Testing 18
    - *a. Dicing of the Si-Al-Si Specimen 20*
    - *b. Test Groove 21*
    - *c. Test Specimen Etching 22*
    - *d. Alternate Method of Preparing Test Specimen 24*
- B. TESTING APPROACH 25
  - 1. Test Conditions 25
  - 2. Loading the Test Specimen 27
  - 3. Testing Apparatus 27
  - 4. Test Apparatus Modifications 29
- C. RESULTS 30

V. CONCLUSIONS 35

LIST OF REFERENCES 37

INITIAL DISTRIBUTION LIST 43

THIS PAGE INTENTIONALLY LEFT BLANK

LIST OF FIGURES

Figure 1. (a) Schematic of Single Layered Cu/PI HDIC on Si. (b) Surface Profile Before and After Thermal Cycling; Plot Representing Differential Deformation of Cu and PI via Sliding at Cu/Ta Interface (From:[7]) 4
Figure 2. Schematic of Interfacial Shear Stress Distribution along a Metal Thin Film Line. (From:[10]) 5
Figure 3. C4 Solder Joints in Flip-Chip packaging. (a) Before Thermal Cycling, (b) After Thermal Cycling 5
Figure 4. (a) Intrusion of Graphite Fiber-Ends after Slow Thermal Cycling; (b) Protrusion of Graphite Fiber Ends after Slow Thermal Cycling (From:[25]) 6
Figure 5. Photo and Schematic of Double Shear Diffusion Bonded Interfacial Creep Test Specimen (From: [3]) 9
Figure 6. Binary phase diagram of Aluminum Silicon systems (From:[54]) 14
Figure 7. Silicon substrate heater and sample holder 16
Figure 8. PVD chamber with attached Diffusion pump 16
Figure 9. Diffusion Bonding Chamber; UC Berkeley 18
Figure 10. Fabricated Test sample for isolating the PVD aluminum thin film interface in single shear 19
Figure 11. Side view diagram of the fabricated test specimen. The aluminum thin film is not drawn to scale 20
Figure 12. Dicing schematic for Si-Al-Si diffusion bonded specimens (From:[55]) 21
Figure 13. K.O. LEE liquid cooled cylindrical grinder/cutter; UC Berkeley 22
Figure 14. Etching apparatus figure(From[55]) and photo 23
Figure 15. (a) Photo is Before Etching (~250 μm to Al Interface); (b) Photo is After 4 Hours of Etching, Showing about 150μm of Si Still Left Between the Groove-Tip and The Al Thin Film 23
Figure 16. Modified design of test sample for isolating the PVD Aluminum Thin film/Silicon interface in single shear. The Aluminum thin film is not drawn to scale 25
Figure 17. Insulative Chamber around Test Specimen 26
Figure 18. The Entire Test Rig Enclosed in the Environmental Chamber 26
Figure 19. Test Apparatus 28
Figure 20. Schematic of Test Apparatus for Single Shear Isolation 29
Figure 21. Interfacial Creep Curves; Various Shear Stresses and Temperatures 30
Figure 22. Average Interfacial Displacement Rate As a Function of Shear Stress, τ 32
Figure 23. Temperature Dependence of Interfacial Displacement Rate with Apparent Activation Energy of ~23.3kJ/mole 33

THIS PAGE INTENTIONALLY LEFT BLANK

LIST OF TABLES

Table 1. Cleaning Sequence for Si Surfaces Prior to PVD of Al thin film.....14

THIS PAGE INTENTIONALLY LEFT BLANK

ACKNOWLEDGMENTS

I thank my mother, Mary Dawson. She did a great job raising me and my sister. My mother was the best example of a hard working person who continuously strove to better herself and the lives of her children. Next, I would like to thank my advisor, Prof. Indranath Dutta. He is a very intelligent professor that took the time to explain and show me how to be a researcher and an engineer. I truly thank him for that. Next, I thank the staff and support unit of the Mechanical Engineering Department. Patty Jackson, Pat Mitchell, Tom Christian, Don Meeks, and Mardo Blanco, have been invaluable. They are extremely over worked, but they continuously found the time to assist me with every problem or casualty to my research. I also would like to thank Dr. Robert Marks. He consistently provided direction that opened my eyes. I could not have had a better person to work with on this research. A final thank you goes to the National Research Foundation for their continued support throughout all of my research.

THIS PAGE INTENTIONALLY LEFT BLANK

I. INTRODUCTION

Advances in the field of microelectronics field have lead to rapid improvements in the performance of devices and packages, but at the same time has resulted in significant complications. Each new development has caused an increase in component density. This is fueled by the desire to have increasingly smaller components and device features in order to provide faster processing capabilities. But with a higher component density at the device scale, come multiple interfaces, which can become critical to the overall performance because of their preponderance in device structures. In a typical multi-layer back end interconnect structure (BEIS), consisting of metal interconnect lines embedded in a dielectric, of a modern microelectronic device, the total area of interfaces may exceed 10^6 m^2/m^3! Clearly, with this much interfacial area per unit volume, the properties of the interfaces often end up controlling the properties and reliability of the entire device.

Microelectronic devices undergo severe thermo-mechanical excursions during service and/or qualification. The excursions can give rise to shear stresses at interfaces between dissimilar materials when there is a significant difference between the coefficients of thermal expansion (CTE) of adjacent materials. If one of the materials adjacent to the interface is subjected to a high homologous temperature (T/T_m), relative movement between the adjacent components may occur via diffusionally accommodated sliding (interfacial creep), even when these components are fully bonded to each other. Clearly this affects the stability and reliability of the entire microelectronic system. Interfacial shear stresses may also be induced during thermal excursions associated with differential thermal expansion/contraction of disparate adjoining components in a microelectronic device/package. Therefore, diffusionally driven interfacial sliding processes can operate in microelectronic devices during both fabrication as well as service.

Funn and Dutta [1] designed procedures to study the kinetics of diffusionally accommodated sliding of interfaces between dissimilar materials. An analytical approach to the study of interfacial creep kinetics in Pb-Ni and Pb-SiO_2 single fiber composites

was the subject of their study. An interface sliding model under the precepts of a diffusional creep law was formulated. The observed stress exponent (n) of unity and the measured activation energy corresponded to interfacial diffusion, diffusional creep controlled by and driven by interfacial shear stresses. In addition, any normal stress acting on the interface was also inferred to influence interfacial sliding kinetics, accelerating sliding when it is tensile, and decelerating sliding when it is compressive. However in this work [1], the impact of normal stresses was not experimentally verified.

Peterson and Dutta [2,3] developed an experimental approach to study interfacial creep in bulk systems of diffusion-bonded interfaces of Silicon and Aluminum. Their research developed a procedure for understanding the interfacial creep phenomenon by relating sliding kinetics with interfacial structure and interfacial stress states (shear as well as normal). The kinetics data recorded from this study enabled them to use atomic force microscopy (AFM) to measure and model the impact of interfacial creep on the reliability of thin film interconnect systems [4,5,6]. Although their experience experimental work on directly measuring interfacial sliding kinetics was based on bulk systems, they reported that thin film-substrate interfaces can also slide via interfacial diffusion-controlled diffusional flow.

The objective of this thesis is to develop a well controlled experimental approach to the study of interfacial creep kinetics of metallic thin film/semiconductor interfaces, which commonly occur in microelectronic devices. A testing methodology was devised and validated and the experimental apparatus was fined tuned. It is the intent of this work to conduct experiments similar to those conducted in bulk Al/Si [2,3] on thin film/substrate interfaces.

II. BACKGROUND

A. EXAMPLES OF INTERFACIAL SLIDING

1. Microelectronics

Interfacial creep is the sliding of components bonded to each other without interfacial de-cohesion (cracking). Interfacial sliding has been observed previously in copper/polyimide high density interconnects (HDIC) on silicon during thermal cycling [7,8]. In this study, which was performed on a Si sample with Cu interconnect lines separated by polyimide (PI) dielectrics (Figure 1a), the surface step height between Cu and PI were found to change after thermal cycling. The Cu-PI and Si-Cu interfaces had Tantalum diffusion barriers in order to maintain the integrity of the Cu interconnect lines.

Atomic force microscopy was used to evaluate the impact on the surface of a single layered Cu/PI HDIC after thermal cycling. Along the vertical Cu-Ta interfaces, sliding was noticed and this sliding resulted in a change in the relative heights of the PI and Cu lines [7,8] (Figure 1b). This sliding was attributed to shear stress driven diffusionally accommodated sliding. The shear stresses were generated by the large CTE mismatch between the Cu, Ta, and PI layers in the out-of-plane direction [10].

Since multi-layered structures typically require successive metal-dielectric layers to be deposited on top of each other [9], during processing of a multi-layered Cu/PI HDIC structures (imidization and Cu deposition), the structure is heated to 350ºC (~$0.45T_m$ of Cu) several times, which subjects the structure to a thermal cycle [10]. If the interfacial step height changes each time a new layer is fabricated, serious flaws can occur in already processed layers thus posing a reliability hazard

Peterson summarizes that the displacements recorded are from one mechanism, interfacial diffusion controlled diffusional creep. He also found that by altering the normal stresses (σ_n) and roughness of the substrate, creep kinetics could be altered. His experimental data confirms that the model proposed by Funn and Dutta [1] is accurate.

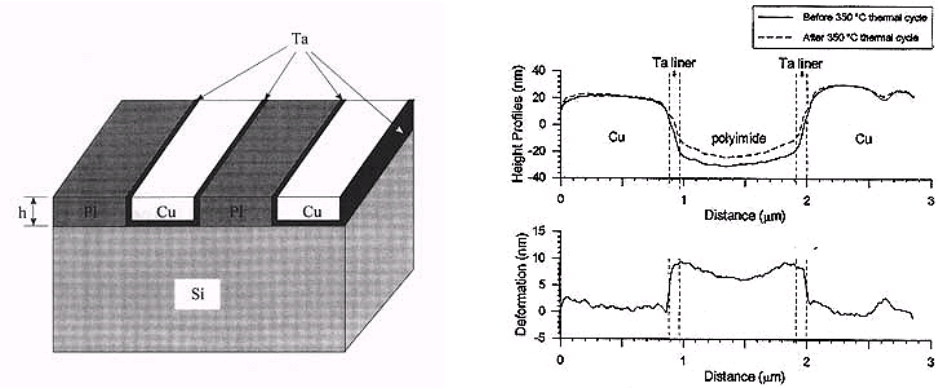

Figure 1. (a) Schematic of Single Layered Cu/PI HDIC on Si. (b) Surface Profile Before and After Thermal Cycling; Plot Representing Differential Deformation of Cu and PI via Sliding at Cu/Ta Interface (From:[7])

Sliding not only occur in the out of plane (vertical) direction, it also occurs in the in-plane horizontal direction [5]. This sliding can be more pronounced than vertical sliding because the metal interconnect lines are not constrained. This, coupled with high stress and temperature, can activate creep mechanisms in the metallic film. Cu films on Si may creep at temperatures as low as 60ºC, and Al films can begin creeping at even much lower temperatures [11,12]. Indeed, in-plane dimensional changes accommodated by interfacial sliding, has been observed after thermal cycling for both Al[13] and Cu [5] thin films on Si.

Figure 2 illustrates the sliding of a thin film of aluminum on Si. The sliding is occurring in the in-plane (horizontal) direction, driven by the interfacial shear stresses which exist at the interface along the edges of the thin film line due to differential cooling of the film/substrate system from the deposition temperature. The in-plane normal stresses in the film cause elastic, plastic and creep deformation of the film, which deforms differently from the substrate. This generates a shear lag at the interface, and produces interfacial sliding, which accommodates the differential deformation of the film with respect to the substrate [13,5]. Interfacial shear stresses which exist mostly near the edges of the film, may be ignored for large area films, because their effect is limited to 1-2 film thicknesses from the film edges [14-17]. But this is the exact opposite for narrow films (e.g., interconnect lines), making the effect of interfacial sliding very important for thin film lines in microelectronics.

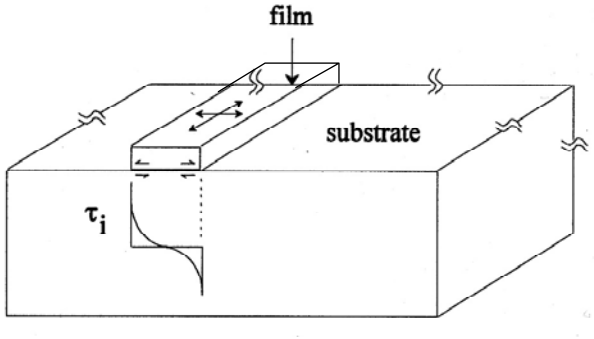

Figure 2. Schematic of Interfacial Shear Stress Distribution along a Metal Thin Film Line. (From:[10])

C4 solder joints, in flip chip packaging, are another area of concern for interfacial sliding. In this microelectronic package, several solder bumps attach a Si device to a Ceramic or organic substrate. The solder bumps, near the edge of the device, are subjected to shear strains due to CTE mismatch between the microchip and the substrate during thermal cycling. Interfacial sliding is a likely occurrence due to the combination of high temperature and shear stresses at the solder/Si and solder/substrate interfaces. [10].

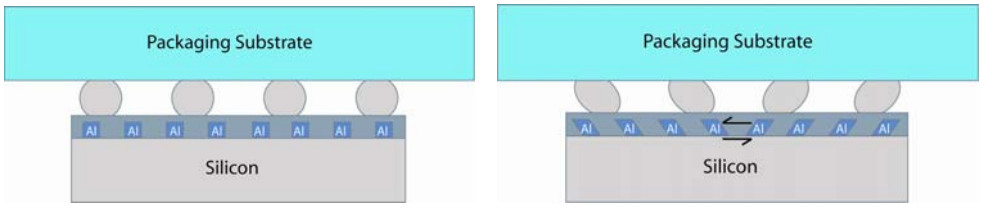

Figure 3. C4 Solder Joints in Flip-Chip packaging. (a) Before Thermal Cycling, (b) After Thermal Cycling

2. Metal-Matrix Composites

The study and understanding of interfacial sliding in Metal-Matrix Composites (MMCs) has become particularly important because of the performance limiting possibilities. Research based on the slow thermal cycling of graphite fiber reinforced aluminum matrix composites [18,19] has revealed that fiber ends either recessed into the matrix or protruded from the matrix ends. This effect was also noted in research involving W fibers in a Cu matrix [20]. The sliding observed in these composites took place without interface de-bonding. This is different from rapid thermal cycling which

interfacial fracture followed by frictional sliding of the de-bonded interface has resulted in relief of residual stresses in the matrix and thus allowed the matrix to shrink in relation to the fibers [21,22]. Interfacial sliding driven by diffusional processes occurs in well bonded interfaces, wheras frictional sliding after failure is common in weak bonded interfaces that undergo thermal cycling. [21-23].

Previous research has developed a model for axial creep with the effect of interfacial sliding [24]. There results showed that sliding was confined to fiber ends. In this experiment, the composite creep rate eventually disappears as the applied load is transferred to the fibers from the matrix. On the contrary, for large fiber diameters and short matrix lengths, sliding may still occur within the gauge length. In this situation, the fiber is still experiencing finite creep rates even after long creep times. An example of this would be in axial creep of turbine blades.[10]

Research on graphite/aluminum composites have shown that fiber ends may protrude or intrude following slow thermal cycling (Figure 6a and 6b) [25]. This experiment showed that intrusion and protrusion can be attributed to diffusionally accommodated interfacial sliding near the ends of the fibers in the composite. A transient deformation mechanism map for thermal excursions was designed based on further analysis.

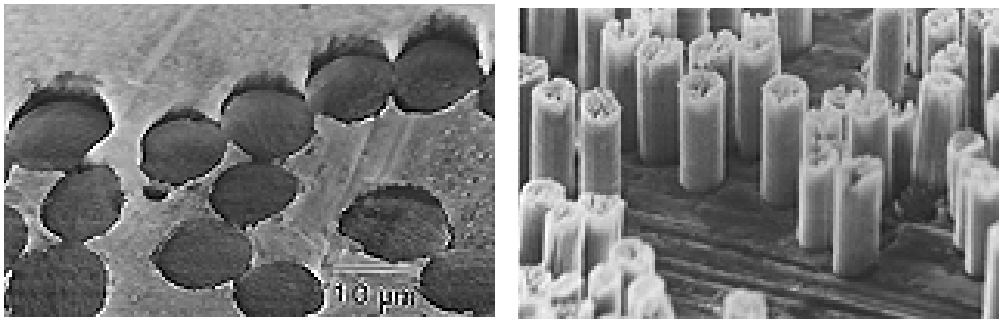

Figure 4. (a) Intrusion of Graphite Fiber-Ends after Slow Thermal Cycling; (b) Protrusion of Graphite Fiber Ends after Slow Thermal Cycling (From:[25])

The above information has explained that the type or chemistry of the interface is presumed to have an effect on its creep rate. It is logical to assume that the structure and chemistry of the interface can play a significant role in its plastic deformation. Also the

mechanism of sliding changes with the shear stress/thermal cycling conditions. Finally, there is no prevailing agreement on the mechanism of these effects but further modeling will aide in this determination. It is easy to understand that interfacial sliding can weaken the structure and ultimately destroy or limit the reliability of a composite system.

B. POSSIBLE MECHANISMS OF INTERFACIAL SLIDING

Interfacial creep is commonly masked by concurrent phenomena. But there has been many systems such as dispersion strengthened metals [26-29], eutectic alloys [30,31], various metal and ceramic-matrix composites [32-35], and film substrate interfaces [36] where indirect evidence of diffusionally accommodated interfacial sliding has been noted. But in none of these cases was interfacial creep studied by isolating it from concurrent and superposed effects [10].

Some previous research has explained interfacial creep by the means of diffusional creep [37]. In this situation the interface is a source and sink for vacancies due to highly mobile boundary/interfacial dislocations (DB) [26,37]. Other research of metallic composites, have designated power-law creep as the source of interface sliding. The interface is believed to be a highly dislocated region that was formed due to a stiffness mismatch between the matrix and fibers. Dislocation loops are forced to stand off from the fibers. The end result is dislocation annihilation which is the catalyst for a recovery process [38-40].

Despite varying opinion of the source of interfacial sliding, the methodologies used to understand interfacial sliding involved measuring overall strain response of a system, subtracting the effects of all known factor, and then attributing the remaining data to interfacial sliding [36,41-43,28-30]. The next method incorporated assuming an interfacial flow law and then modeling a system according to that law. Finally, the experiments conducted would be compared to analytical results [44-49]. But as expected it is difficult to isolate and study the kinetics of interfacial sliding using the above methods.

Funn and Dutta [1] have described interfacial sliding by a diffusional creep law. They designed an approach that would isolate interfacial creep kinetics from other

mechanisms of interfacial sliding, which is controlled interfacial diffusion. They proposed that interfacial-diffusion-controlled diffusional creep, combined with shear and normal stresses, is the driving force for interface sliding, which is controlled by interfacial diffusion. Since interfacial diffusion can be quite rapid, interfacial sliding may be significant even at fairly low temperatures..

C. DIRECT MEASURMENT OF INTERFACIAL CREEP KINETICS

Funn and Dutta isolated and measured the kinetics of interfacial sliding of the matrix-fiber interface.[1]. They concluded that in addition to the shear stress, the interfacial normal stress also influences diffusional flow along the interface, and that surface morphology affected the stress state of the entire system, threby having a strong influence on the kinetics of sliding.

Their study used two model, single fiber composite (SFC) systems. The first model had a system with no mutual solubility (Pb-matrix/ quartz fiber) and the second model had limited mutual solubility (Pb-matrix/ Ni fiber). For both systems, the method of sliding was believed to be interface diffusion-controlled diffusional creep. The low Q levels displayed and the very small applied shear stresses led to this conclusion, because dislocation climb could be eliminated. After SEM analysis of the interfaces; the topography was viewed to be consistent with the idea of local normal stress variation. This variation was along the interface and believed to be generated by a globally applied shear stress. The kinetics of this stress are illustrated in the below equation.

$$\dot{\gamma}_{\mathrm{i}} = \frac{4\delta_{\mathrm{i}} \mathrm{D}_{\mathrm{io}} \Omega}{\mathrm{kTh}^3}\left[\tau_i + 2\pi^3\left(\frac{\mathrm{h}}{\lambda}\right)^3 \sigma_{\mathrm{i}}\right] \exp\left[-\frac{Q_i}{RT}\right] \qquad (2.1)$$

τ_i is the shear stress acting on the interface, Q_i is the activation energy for the interface, D_{io} is the interface diffusivity, Ω is the atomic volume of the diffusing species, δ_i is the

thickness of the interface, λ is the periodicity of the interface and **h** is the width of the interface. σ_i is the stress acting on the interface and **k**, *R*, and *T* are the Boltzmann constant, gas constant and the absolute temperature respectively.

In the above equation, the shear and normal stresses are the driving forces of interfacial sliding. When this is coupled with surface roughness (h), the effect will either increase the rate with smoother surfaces or decrease the rate with rougher surfaces. The surface roughness, of current generation microelectronic devices, is at the Angstrom level. This fact alone makes such devices more susceptible to interface sliding.

Peterson, Dutta and Chen [3,10,50] performed direct measurements of interfacial sliding on an isolated Al/Si diffusionally bonded interface. They loaded a diffusionally bonded specimen of Al-Si-Al in double shear to study and measure the interfacial creep kinetics along each diffusion bonded interface (Figure 5)

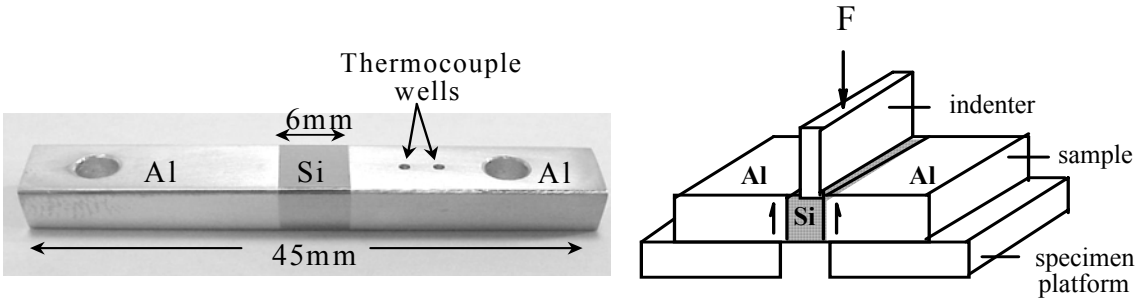

Figure 5. Photo and Schematic of Double Shear Diffusion Bonded Interfacial Creep Test Specimen (From: [3])

With their results, they validated the interface diffusion controlled diffusional creep model for interfacial sliding. They also showed that creep rate decreases with increase of interfacial roughness, and that during the experiments, all deformation of the sample was confined to the interface. This was noted with no interfacial de-cohesion. Finally, the application of a far field normal stress produces a threshold stress, which also depends on the interfacial topography (h/λ), and can either accelerate sliding (for tensile normal stresses) or decelerate sliding (for compressive normal stresses). Peterson's experiments [10] were carried out on diffusion-bonded interfaces between bulk Al and Si, where, a 20-30 nm thick amorphous zone that was observed to exist at the interface, was

believed to serve as a short circuit path for interfacial diffusion. Since thin Al film/Si interfaces may not have this amorphous layer, it is important to conduct experiments to evaluate the role of interfacial sliding at there interfaces.

III. OBJECTIVE

The objective of this research is to develop a methodology to analyze the kinetics of interfacial creep at the thin Al film and a silicon substrate. In order to accomplish this objective, a strategy was devised in order to isolate deformation at the Al thin film/silicon interface from other concurrent deformation processes (e.g. creep of Al film) through a combination of sample and test approach design. Therefore the goals of this thesis are to; (1) design a sample conducive to testing sliding at thin film/substrate interfaces, (2) devise a test methodology which is amenable to testing such samples, and (3) obtain example creep curves to demonstrate the viability of the proposed approach.

THIS PAGE INTENTIONALLY LEFT BLANK

IV. PROCESSING AND CHARACTERIZATION OF DIFFUSION BONDED Al-Si INTERFACES

A. EXPERIMENTAL PROCEDURE

1. Materials

Single crystal silicon was used as the substrate material for our test samples because of its frequent use as a substrate material in microelectronic devices. The silicon was 99.999+% pure and had the <100> direction pointing normal to the substrate surface. Single crystals with a <100> orientation were selected in order to be consistent with microelectronic device applications, as well as because the chemical milling procedures with were necessary for sample fabrication are well characterized for this direction [51-53]. The Al thin film was 99.9% pure and was deposited on Si via vacuum evaporation. The Al/Si system was chosen to serve as a model system for studying interfacial sliding, since Al and Si show very limited mutual solid-solubility below the eutectic temperature (850 K), thereby being able to produce a reasonably sharp interface. The phase diagram below illustrates this (Figure 6).

At the eutectic temperature (850 K), approximately 1.65wt% of Si dissolves in aluminum, whereas the maximum solubility of Al in Si is only 0.5wt%. Therefore, if during processing, the maximum temperature is kept below 850 K, very little of the Al is expected to dissolve to Si, allowing the interface to be relatively sharp.

2. Sample Preparation

a. Sectioning, Polishing, and Cleaning

Thirty pieces of silicon (25.4 x 25.4 x 3.5 mm) were cut from an ingot of silicon to ensure that each sample had a <100> orientation. Each piece was then lapped to a flatness of < 1º/ inch and polished to a 0.05 μm finish on one side in preparation for diffusion bonding. Next a series of cleaning steps designed to degrease and deoxidize the surface of the silicon blocks was performed. Table 1 explains the sequence.

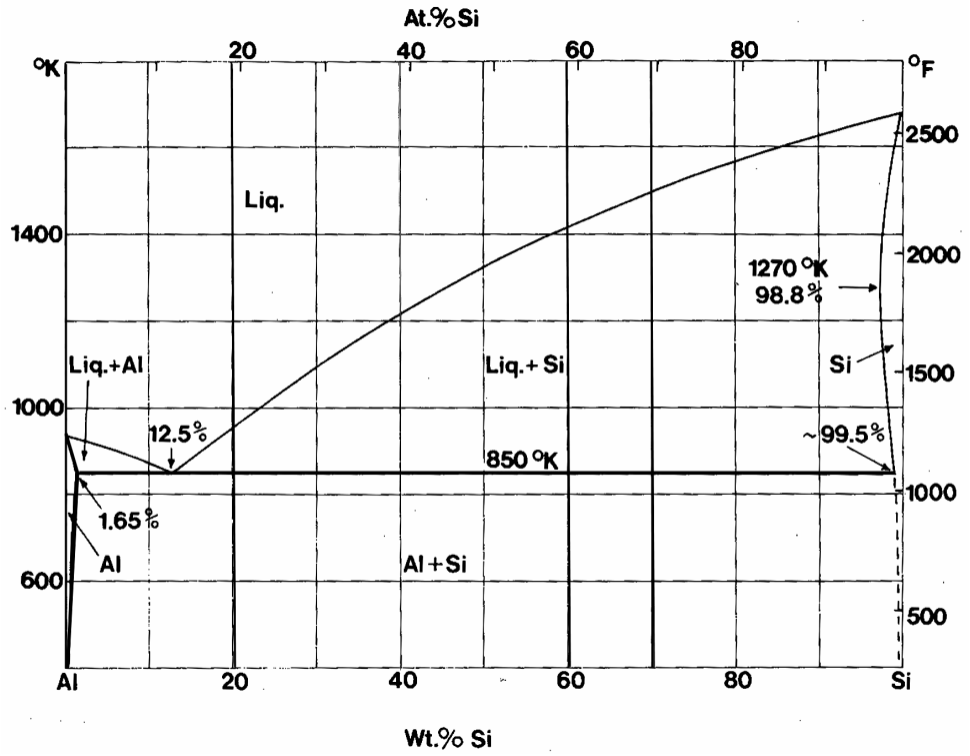

Figure 6. Binary phase diagram of Aluminum Silicon systems (From:[54])

1	2	3	4	5	6	7
Acetone Degrease	2 Propanol Degrease	De-ionized H_20	10% HF De-Oxidize	De-ionized H_20	2 Propanol Rinse	Hot Air Dry
10min	10min	5min	45sec	5min	45sec	2min

Table 1. Cleaning Sequence for Si Surfaces Prior to PVD of Al thin film

The Aluminum pellets used for Al thin film deposition were prepared by first removing its oxide layer. Each piece was polished with 800 grit and 1000 grit silicon carbide paper. The aluminum pellets were then sectioned into 4 equal parts and stored in a 50 ml beaker of 2 Propanol. Proper polishing of the aluminum chips allowed a clean surface to be exposed for more efficient sublimation.

b. Vacuum Evaporation of Aluminum

Physical Vapor Deposition (PVD) was used to form the metallic thin film on the polished Si surface. This procedure began by filling two Tungsten wire baskets

with cleaned, polished and sectioned pieces of Aluminum. The polished silicon wafers were attached to a heated sample holder (Figure 7) and placed in the PVD vacuum chamber (Figure 8) The PVD chamber was drawn down to a vacuum of $5x10^{-8}$ torr. The Si temperature was then increased to 573 K and held at that temperature for 2 hours. This was an annealing measure to remove any residual surface contamination. The Si temperature was decreased to 428 K. Once the temperature stabilized, vacuum evaporation was initiated.

While the substrate was held at 428K, current was applied to the tungsten baskets at 1Ampere (A) per minute until 25A of current were achieved. At this point the current was raised at 1A intervals every 15-20 seconds until 30A were achieved. It is important to keep close watch of the amperage applied to the tungsten coils. As the aluminum chips settle in the basket, the current across the basket can quickly spike to over 50 amperes. When this happens one must decrease amperage to prevent breaking the tungsten baskets and damaging the current leads that are attached to the tungsten baskets. Current was maintained until at least 1μm of aluminum film was deposited onto the silicon surface. Film thickness level was measured by an ultrasonic film thickness monitor. The thickness monitor used an oscillation crystal to determine the amount of metal deposition. As the amount of deposited aluminum increased the vibrating resonance of the disk would change accordingly.

When properly cleaned and polished chips of aluminum were placed in the tungsten basket for deposition, over 1μm of aluminum could be deposited onto the silicon substrate from each tungsten basket. Good engineering practice while heating the tungsten basket must be maintained. The probes holding the tungsten basket were maintained slightly loose. This allowed for heating expansion; which subsequently maximized the life of the tungsten baskets and allowed for high levels of metal deposition.

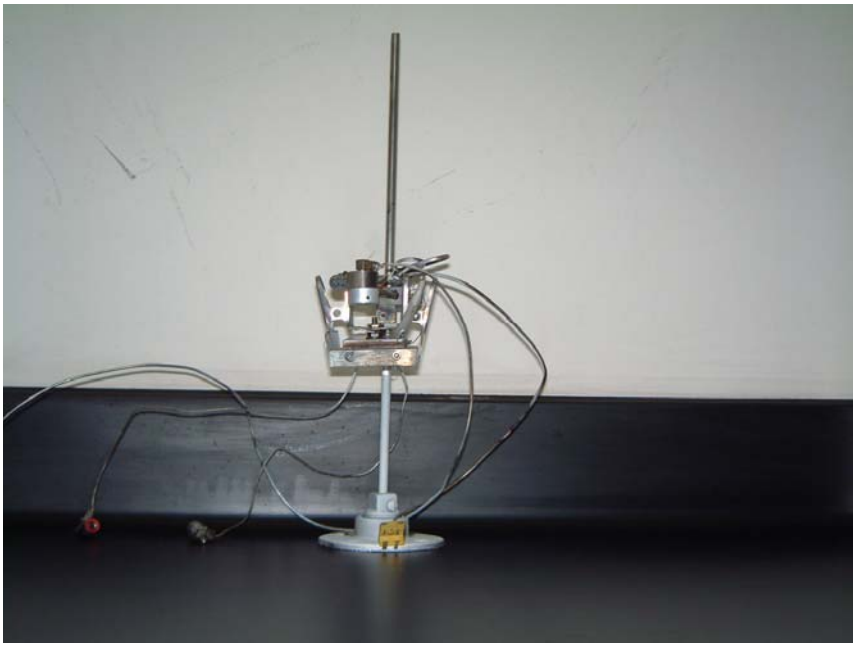

Figure 7. Silicon substrate heater and sample holder

Figure 8. PVD chamber with attached Diffusion pump

Once metal film deposition was completed the silicon substrate was heated to 623 K for 15 minutes. This second annealing time was utilized to stabilize the new film microstructure. The Si was then slow cooled to room temperature (6 K per minute).

Once cooling was completed, the polished side of a second piece of Si was placed onto the Al film and the Si-Al-Si sandwich was immediately wrapped in Al foil and placed in a desiccant chamber under vacuum until it could be placed in the diffusion bonder. This was done to minimize oxidation of the substrate.

3. Diffusion Bonding

To complete the fabrication of our test specimen, the second cleaned and polished Si block was diffusion bonded to the vacuum evaporation aluminum thin film. The orientation of vacuum evaporation substrate to non-vacuum evaporation substrate was monitored during placement into the diffusion bonder. It is important to know the orientation of the sample so as to identify the PVD interface from the diffusion bonded interface for subsequent testing.

The diffusion bonding of the Si-Al-Si sandwich was accomplished at the University of California, Berkeley, with the assistance of Dr. R.A. Marks. The Si-Al-Si specimens that were wrapped in Aluminum foil were placed between graphite cylinders (approximately 50.8mm in dia.). The cylinders (with the specimen between) were then placed into the vacuum chamber of the diffusion bonder (Figure 9). Once the cylinders were aligned with the hydraulic ram inside the vacuum chamber, the radiant heater was raised to place the specimen precisely in the middle of the radiant heater. The chamber was sealed and the specimen was placed under 7 MPa of pressure. Once that was completed, the vacuum chamber was drawn down to 5×10^{-5} torr. During vacuum draw-down, the pressure is monitored to ensure that its level is maintained. Once the vacuum pressure was achieved, the specimen was heated at 2 K per minute until it reached 843 K. The temperature was monitored closely to ensure that the eutectic temperature was not crossed. Once thermal conditions were met, the sample was held at this point for 2 hours. After the bonding time was completed, the specimen was slowly cooled to room temperature over a period of 4 hours and then unloaded. The pressure was monitored during specimen cool-down to prevent over-loading of the sample.

Many bonding runs were performed in order to optimize the appropriate bonding stress. It was found that specimens placed under stresses less than 7 MPa produced smaller regions of bonded area. On the other hand, if the pressure exceeded 7 MPa multiple stress cracks propagated through the specimen.

Figure 9. Diffusion Bonding Chamber; UC Berkeley

4. Mechanical Design for Testing

In designing specimens for testing, attention was paid to the thickness of the thin film in order to ensure that it correlates to typical film thicknesses found in microelectronic devices (~ 1μm). Another important requirement is overall test specimen size. Although most microelectronic devices have very small film/substrate interface areas for individual interconnects, the very small load requirements for testing such interfaces is very difficult to satisfy with conventional equipment. Therefore large interfacial areas (~6mm x 6mm) were used in the present samples. Each test specimen was a Si-Al-Si sandwich with a one micron aluminum thin film deposited in the middle.

The test specimens formed became a ~6mm x 12mm test block (Figure 10), with the Al film having two 6mm x 6mm interfaces with the Si blocks on either side. The interfacial region interest was located between two grooves cut/etched into the Si blocks at either side of the Al film. Although the sandwich specimen has 2 Al/Si interfaces, by cutting/etching one groove in the Si up to the Al film, and the other cutting/etching through the Al film, as shown in Figure 7, the sample was capable of leaving only one of the interfaces in shear. By cutting/etching the grooves appropriately, it would then be possible to load only the PVD interface (as opposed to the diffusion bonded interface) in shear.

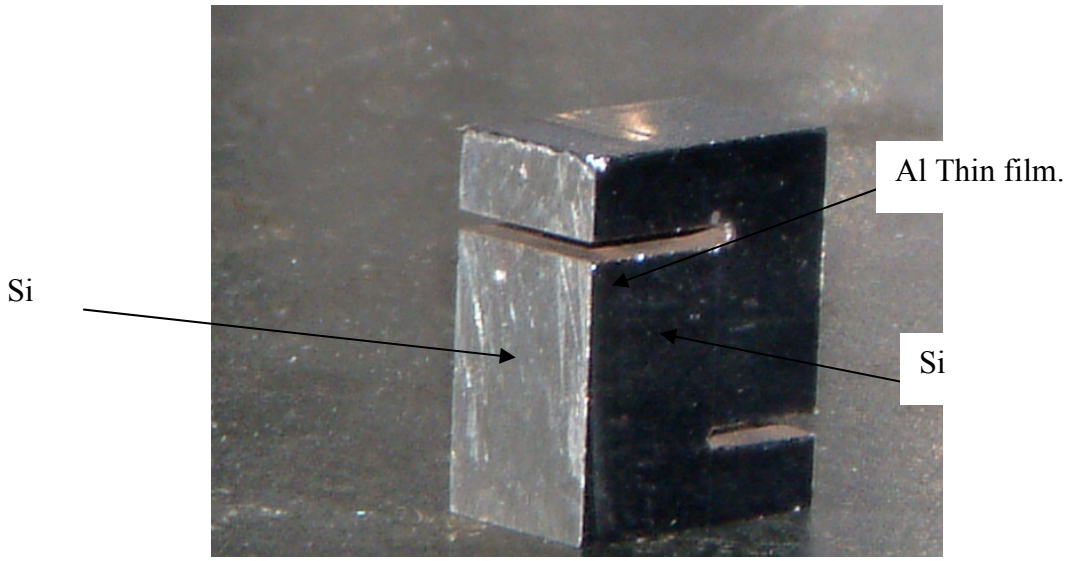

Figure 10. Fabricated Test sample for isolating the PVD aluminum thin film interface in single shear

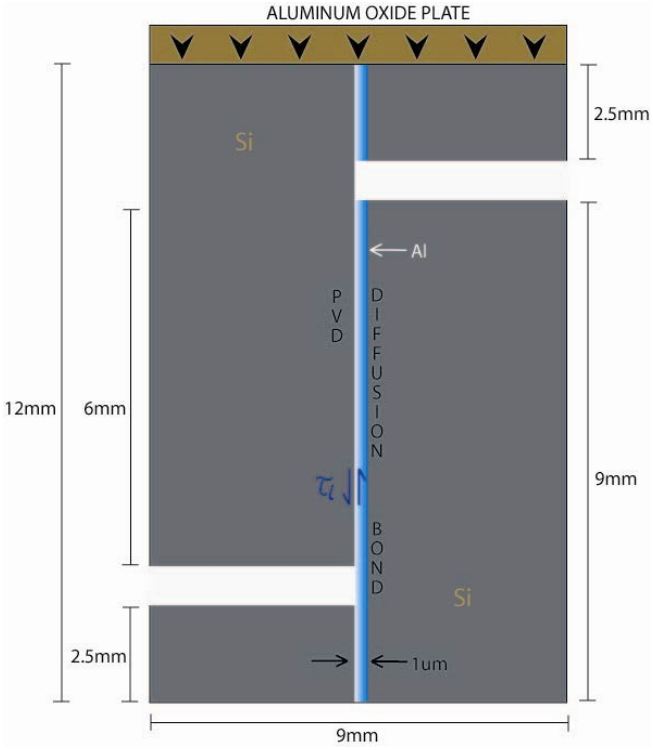

Figure 11. Side view diagram of the fabricated test specimen. The aluminum thin film is not drawn to scale

a. Dicing of the Si-Al-Si Specimen

A slow speed diamond saw was used to dice the Si-Al-Si specimens into testable pieces. Originally there was a dicing plan that would utilize the majority of the specimen bonded area. Figure 12 shows the dicing plan. But this was a very optimistic approach. The best specimen yielded 4 test samples instead of the intended 8.

Each composite sandwich was mounted to a glass plate for dicing. The dicing would begin on one edge of the specimen until an area of good bonding was reached. This procedure was conducted on all four sides. Once this was done on all four sides; the specimen could be diced into ~12mm x ~6 mm test samples.

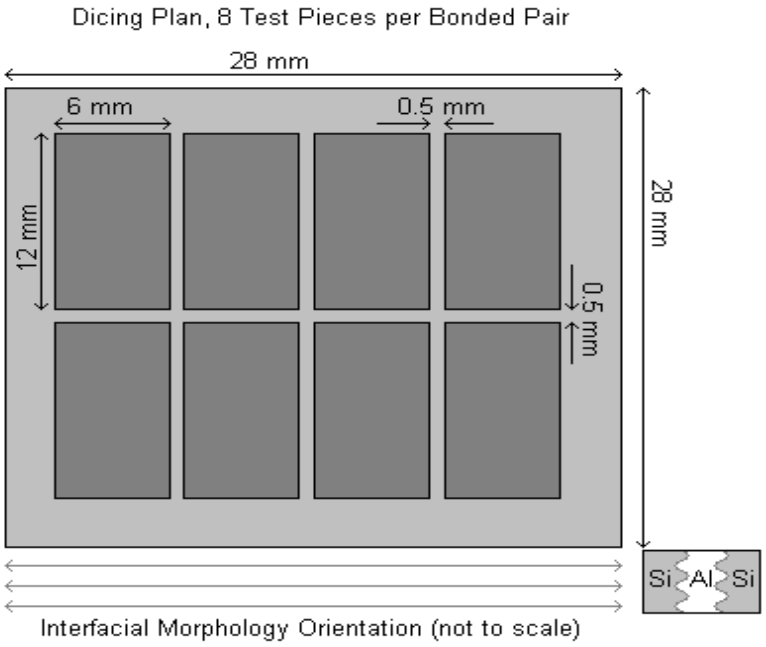

Figure 12. Dicing schematic for Si-Al-Si diffusion bonded specimens (From:[55])

b. Test Groove

Cutting test grooves into each test specimen was performed in 2 different ways. One method used a cylindrical grinder/cutter utilized at U.C. Berkeley (see Figure 13). This saw could cut to within 10-20 μm of the vacuum evaporated interface. The second method utilized was a slow speed diamond saw. This procedure was less accurate and could only be utilized to within ~ 200 μm of the interface, but because it was more readily available, it was used more frequently.

Figure 13. K.O. LEE liquid cooled cylindrical grinder/cutter; UC Berkeley

c. Test Specimen Etching

Etching of the test specimen proved to be the most difficult procedure of specimen fabrication. A more precise procedure for etching is still being investigated. A chemical milling procedure must be utilized due to the hazard of damaging the vacuum evaporated interface from mechanical cutting.

To begin the anisotropic etching of the silicon test specimen, TetramethylAmmonium Hydroxide (TMAH) was used to mill the Si remaining between the tip of the groove and the Al film down to the aluminum interface. This chemical, under appropriate test conditions was found to etch <100> silicon at an accelerated rate. Research in this area [51] developed the proper chemical composition of TMAH with certain basic additives to produce a chemical milling solution that would properly etch silicon (~0.9-1.0μm per minute), but not attack the aluminum thin film (0μm per minute). The chemical composition recommended to maximize Si etch rate while minimizing Al etch rate was: 5 wt% TMAH $(CH_3)_4NOH$, 1.6 wt% dissolved silicon (Si) and 0.5 wt% Ammonium Peroxidisulfate $((NH_4)_2S_2O_8)$. The silicon powder had to be completely dissolved into the 5 wt% TMAH (at 313-323 K) before adding the remaining addictives and when the etching temperature of 358 K was strictly adhered too, the best etching rate of 1μm per minute was achieved.

The chemical milling methodology utilized placing each test specimen in a 50 ml beaker while slowly stirring the heated etching solution. Test specimen holders were fabricated out of Teflon to reduce damage of test specimen from solution rotation/volatility. Despite attempts of perfecting the etching process, the desired silicon etching rate of 0.9-1.0μm per minute was never achieved. The best etching rate obtained in our laboratory was 0.1μm per minute. Figure 14 shows the apparatus used to heat and stir the etching solution. Figure 15 shows before and after views of the chemical milling process.

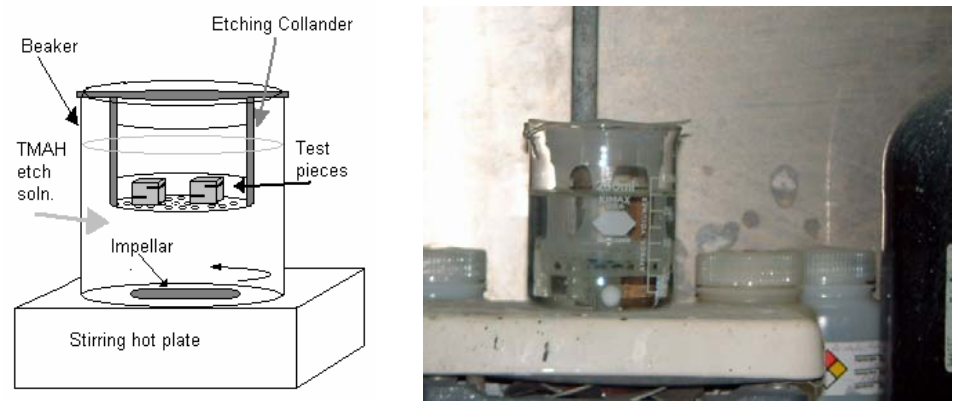

Figure 14. Etching apparatus figure(From[55]) and photo

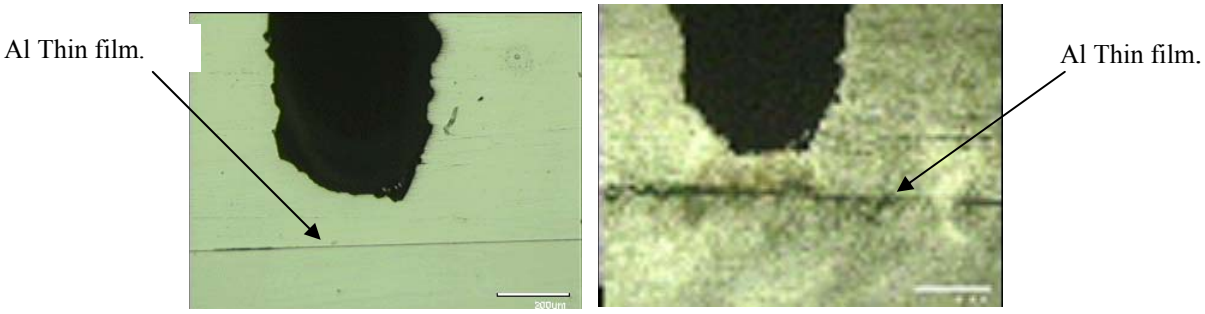

Figure 15. (a) Photo is Before Etching (~250 μm to Al Interface); (b) Photo is After 4 Hours of Etching, Showing about 150μm of Si Still Left Between the Groove-Tip and The Al Thin Film

The etching process employed presented many obstacles. The width of each groove (~0.5 mm), potentially formed a capillary, which coupled with the strong surface tension between the liquid TMAH and the Si, prevented proper circulation of the

liquid at the groove-tip. Because of lack of circulation, the liquid at the groove tip got saturated with dissolved Si early on, and inhibited further etching. Spinning of the etching solution and sonic vibration of the etching solution still did not produce adequate etching inside the groove. A thin layer of SiO_2 was expected (10-20 angstroms) [51,56], plus] on the surface of each test specimen; so before each etching, the notch was carefully cleaned with 800 grit silicon carbide paper and a diamond wafering blade. Yet, the obtained etching rate was ~ 0.1μm per minute.

These complications did not allow for the proper fine tuning of the chemical milling process in the available time. Possible reasons for this difficulty are thought to be related to the amount of SiO_2 growth on each test specimen and the lack of proper continuous flow of etchant through each groove of the test specimen.

d. Alternate Method of Preparing Test Specimen

To circumvent the above complications, an alternate method was formulated. A slow speed saw was used to cut both notches of the specimen approximately 200μm beyond the PVD interface. 800 grit silicon carbide paper was utilized to clean the groove after cutting, as shown in Figure 16. This geometry loads both PVD and diffusion bonded interfaces, as well as the intervening Al thin film, in shear. This method brings into concern the possibility of deformation of the aluminum film, which would get added to the overall observed interfacial displacement. However, strain expected in the Al at a stress τ = 1 MPa, and temperature T =623 K, showes that for a film thickness h = 1μm, the shear displacement of the Al film is $\delta = h\dot{\gamma}_{Al}t$ ~ 0.01μm, where t is the time of a typical creep test (~ 12 hours), and is the steady state shear creep of Al and deemed not have a significant effect on the interface sliding rate (0.01 μm). $\dot{\gamma}_{Al}$ is given by [57].

$$\dot{\gamma}_{Al} = A \times \left(\sqrt{3}\right)^{n+1} \frac{(Gb)}{(kT)} \left[\frac{\tau}{G}\right]^{n} D_{Ov} \times e^{-\frac{Q_v}{RT}} \qquad (4.1)$$

Where A is the Dorn constant, **G** is the shear modulus, **b** is the Burgers vector, **k** Boltzman's constant, **T** is temperature in Kelvin, τ is the shear stress, $\mathbf{D_{ov}}$ is the

Diffusivity of Aluminum, Q_v is the activation energy of Aluminum, and R is the universal gas constant in J/mol-K. Since δ = 0.01μm, this is well below the total measured creep displacements, and the resolution limit of our displacement measuring system, therefore it was deemed that the measured displacements represented only interfacial displacement.

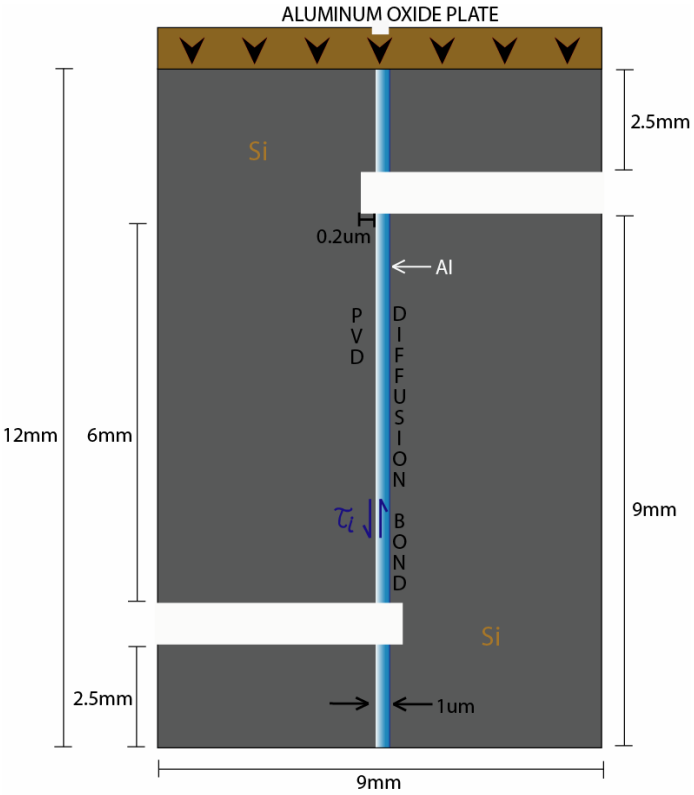

Figure 16. Modified design of test sample for isolating the PVD Aluminum Thin film/Silicon interface in single shear. The Aluminum thin film is not drawn to scale

B. TESTING APPROACH

One of the objectives of this thesis is to validate the kinetics of interfacial sliding of Al thin film/Si substrate interfaces. This validation requires a test methodology and apparatus that will properly isolate the interface between the vacuum evaporated thin film and the Si-substrate, so that the sliding rate at this interface can be determined.

1. Test Conditions

There are two conditions that must be maintained for proper analysis of interfacial sliding kinetics. The first is a steady high homologous temperature and the second is a

steady load even as the sample has begun to slide in response to the applied load. Since the extent of interfacial sliding is expected to be small during our experimental (i.e., the measured displacements are ~ 2-3 μm), it is deemed important to keep the load constant to within ± 0.2 N, and the temperature constant to within ± 0.1K, so that load and temperature fluctuation do not show up as displacement fluctuation in the creep curves.

The temperature was controlled by utilizing two radiant heaters that were placed in close proximity to the testing specimen. The specimen was placed in a specially designed holder. To maximize a thermally stable environment, an insulative chamber, consisting of Fiberfrax (Short Staple Ceramic Fiber) board wrapped in Al foil, was built around the sample holder and the heaters, as shown in Figure 17. This chamber was then placed inside of an environmental chamber, which served as an additional thermal insulation in order to limit the effects of environmental temperature changes (Figure 18).

Figure 17. Insulative Chamber around Test Specimen

Figure 18. The Entire Test Rig Enclosed in the Environmental Chamber

2. Loading the Test Specimen

Each sample was loaded depending on the level of stress required for (Al) testing. A test range of 0.5-2.0 MPa was utilized. The interfacial area of each test specimen was measured for each specimen prior to testing, and with equation 4.2, the amount of force in Newtons (N), required was calculated for the desired stress interfacial shear strain state τ_i.

$$F = \tau_i \, \mathbf{A}_i \tag{4.2}$$

Since most of the samples interfacial areas were ~6mm x 6mm, the nominal load requirement for every 0.5 MPa of shear stress was ~ 18 N. An MTS TestStar IIs system was used to conduct the experiments under load control, in order to maintain a constant load throughout the entire test. The load control system was coupled with a 2224 N load cell.

Multiple creep tests were performed on each sample at prescribed temperatures. A program was generated that could perform this task without monitoring. Each creep test would run for 12 hours at a set stress state. Upon completion of the 12 hour run, the program would increase the stress state to the next desired level and then hold this level for 12hours. This procedure could be repeated as many times as desired. Four creep tests were the most performed on any test specimen for this thesis.

3. Testing Apparatus

The testing apparatus was designed specifically for this test sample. Most of the test rig was fabricated from INCONEL X750, in order to limit the impact of thermal expansion mismatch between disparate materials during testing. Figure 14 illustrates the testing apparatus.

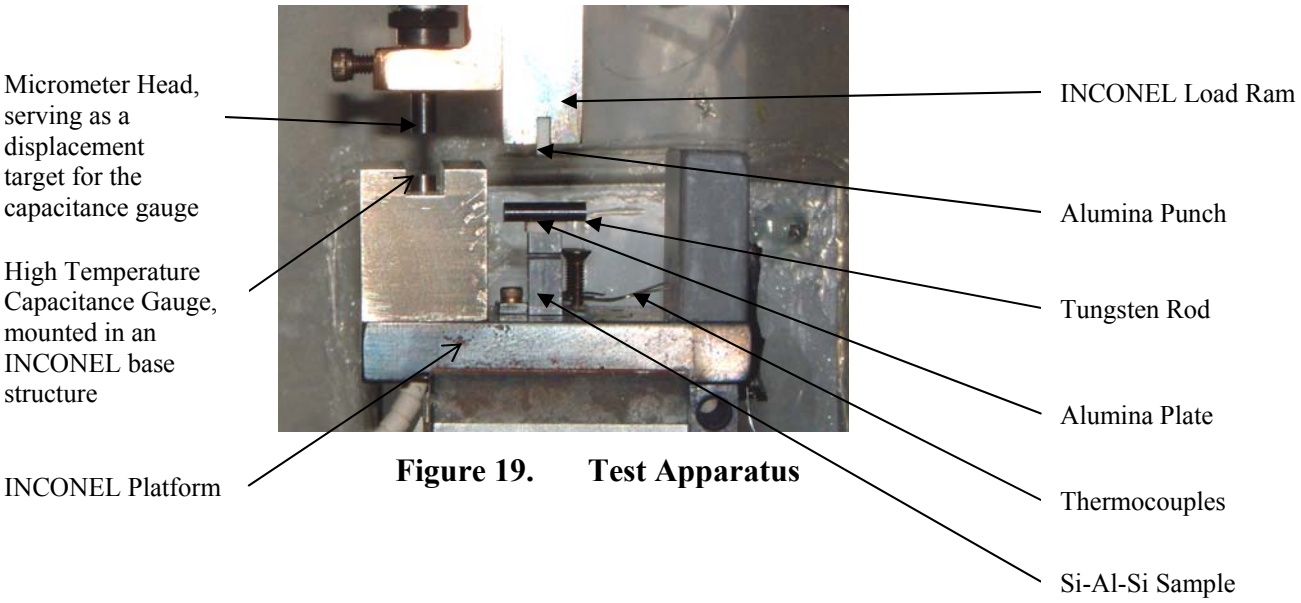

Figure 19. Test Apparatus

The basic test rig consisted of an INCONEL sample platform with a spring loaded arrangement to hold the sample in place. Attached to which is an INCONEL base structure in which a high-temperature capacitance gauge, clad in INCONEL is mounted. An alumina plate was placed on top of the sample in order to apply a uniform pressure to the entire top surface of the sample during experiments. A tungsten rod (pin) was then placed on the alumina plate. The load rod, which was also made of INCONEL, had an alumina punch mounted on it and this was used to apply load on the tungsten rod. A micrometer attached to the load rod was used as the target for the capacitance gauge to measure the displacement between the fixed load rod, and the moving ram to which the specimen stage is attached, as creep progressed. A schematic of the experimental arrangement is shown in Figure 20.

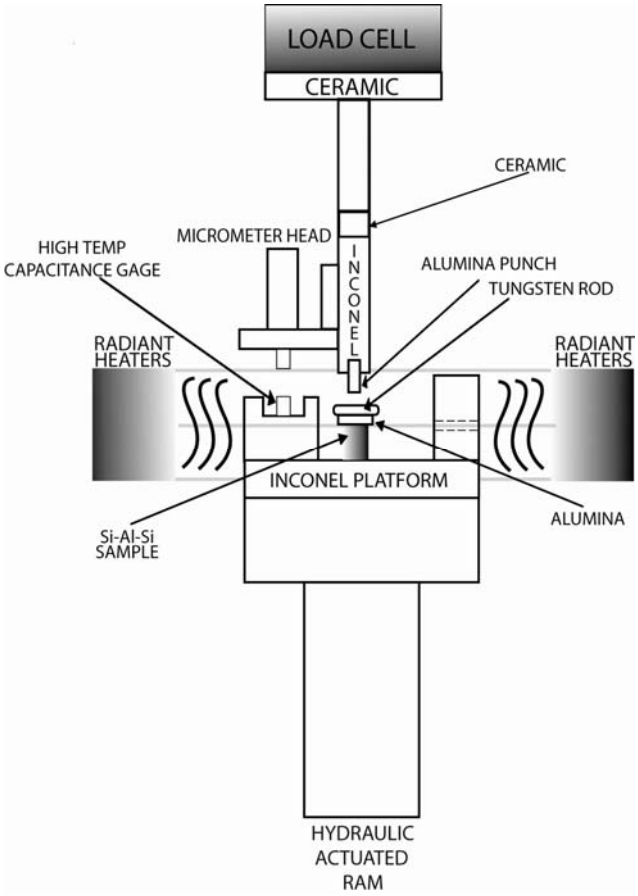

Figure 20. Schematic of Test Apparatus for Single Shear Isolation

4. Test Apparatus Modifications

A few adjustments were made to the testing apparatus in order to obtain the creep curves, which resulted in very small total displacements, and hence were highly sensitive to even slight temperature fluctuations at the load cell, which resulted in detectable load variations due to zero-shift errors. Data analyzed after several testing runs showed a large effect from temperature fluctuation of the load cell. To limit this effect a more active temperature control of the load cell was attempted. Cooling coils were placed around the load cell, with the temperature of the coils being maintained at 0ºC using a NESLAB Endocal Refrigerated Circulating Bath system. The NESLAB was monitored for accurate temperature regulation and was utilized throughout each experiment. An insulation wrap of fiber glass was placed around the entire load cell/coil system. This limited the effects of environmental fluctuations.

C. RESULTS

Figure 21 shows some of the creep curves obtained from the interfacial creep tests. In Equation 2.1, the shear stress applied, τ_i, is the driving force for interfacial sliding. It is apparent from the illustration that with an increase in applied shear stress, there is an increase in steady state displacement rate. As seen from the figures, the displacement rate reaches a steady state within ~ 2 hours for all the stress and temperature conditions. It should be noted that the instantaneous displacements obtained immediately after loading the sample to the creep stress are not accurately reflected in the figure, since multiple tests were conducted on each sample, and the instantaneous displacements were subtracted off from the creep curves prior to plotting.

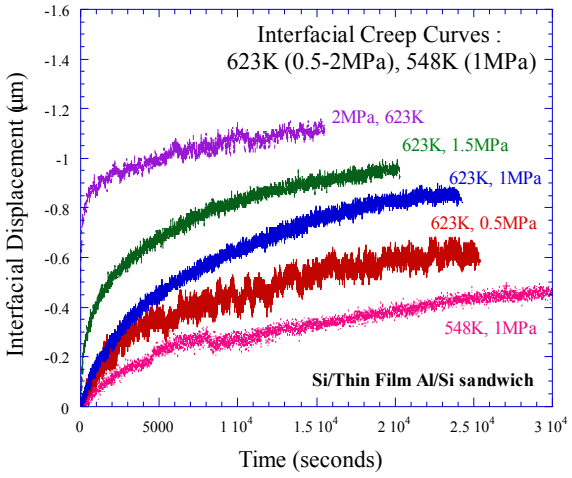

Figure 21. Interfacial Creep Curves; Various Shear Stresses and Temperatures.

The experiments were performed on the vacuum evaporated Al film our of Si-Al-Si sandwich. The film was deposited up to ~1um of thickness. No normal stresses were applied during testing and no predicted compressive stresses were believed to exist during testing. The shear stress, τ_i, and the temperature were the only parameters varied during testing. Figure 22 is a plot of the average interfacial displacement rate ($\dot{\bar{U}}$) as a function of the applied shear stress, τ_i. In this figure the interfacial displacement rate,

$\dot{\bar{U}}$, is proportional to the applied shear stress, therefore n (slope) ~1. The displacement rate displays a linear stress dependence for the entire temperature range (0.51 T_m – 0.67 T_m), but the creep rate does not vanish at zero stress. The graph illustrates a linear shear stress dependence, but with a noticeable threshold stress (τ_o) observed even though no normal stress was applied during testing. In the present test procedure, the interfaces were nominally loaded in shear only. However, as noted in equation 2.1, this would not give rise to a threshold stress, which can only exist if the interface is loaded in compression as well. In the present sample geometry, it is unclear how this compression could have arisen, although because of the complicated sample and loading geometries, it is not unreasonable that there is some compression as well as shear on the interfaces during loading. Therefore, it is inferred that the stress state of the interfaces is not simple shear, but because of complications due to specimen geometry and loading conditions, there is also a compressive normal stress at the interface, which causes the observed threshold, stress. Further testing with this specimen geometry, coupled with finite element modeling of the loading state, are recommended for future work in order to determine the origins of the threshold stress recorded

Figure 23 shows a plot of $\ln\dot{\bar{U}}$ vs 1/T for the applied stress of 2 MPa. This plot gives an apparent activation energy (Q_{app}) of 23.3 kJ/mole. Previous research with Al/Si interfacial creep [10], showed that diffusionally accommodated interfacial sliding of an Al/Si interface had an activation energy of ~42kJ/mole. This was attributed to diffusion of Al atoms through a narrow amorphous core (~ 20nm thick) along the interface, under the influence of short range stress gradients along the interface. The Q_{app} measured in this work is even lower than the activation energy of diffusion through amorphous aluminum. It is not totally understood why there is such a disparity in values, but again, it may be related to complications due to specimen geometry and loading states, possibly resulting in low observed value for Q_{app}. What may be occurring is that the displacement due to both interfaces is being recorded, and the two have different temperature dependencies. If one of the interfaces could be isolated and then data recorded, this may show a higher Q_{app} value. Another possibility is the measured displacement not only includes the displacements at the two interfaces, but also that of the aluminum thin film

between the two A/Si interfaces. However, as discussed earlier (Experimental Procedure; A,4,d), the deformation due to Al is expected to be minimal compared to the measured displacements, as computed using equation 4.1 [57]. The value calculated was ~0.01μm, which is far below our recorded displacement resolution. Therefore, it is unlikely that the deformation of Al has influenced the measured readings. Furthermore, since the activation energy for creep in Al is expected to be between ~ 80-142 kJ/mole (for grain boundary/core diffusion and volume diffusion, respectively), it would only bias the measured activation energy upwards. Therefore, we conclude that deformation of the Al thin film is not an issue in the present tests, and the observed low value of Q_{app} is either a real effect, or is associated with complications in the loading state/specimen geometry. Further investigations, and complementary finite element modeling studies to understand these effects are necessary in the future.

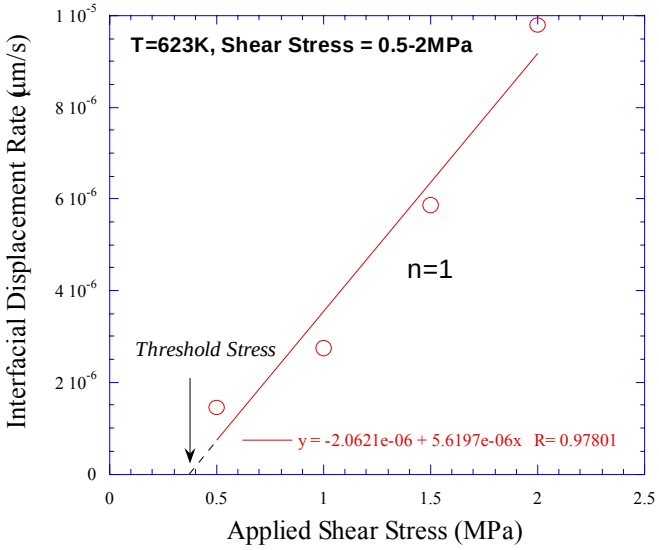

Figure 22. Average Interfacial Displacement Rate As a Function of Shear Stress, τ

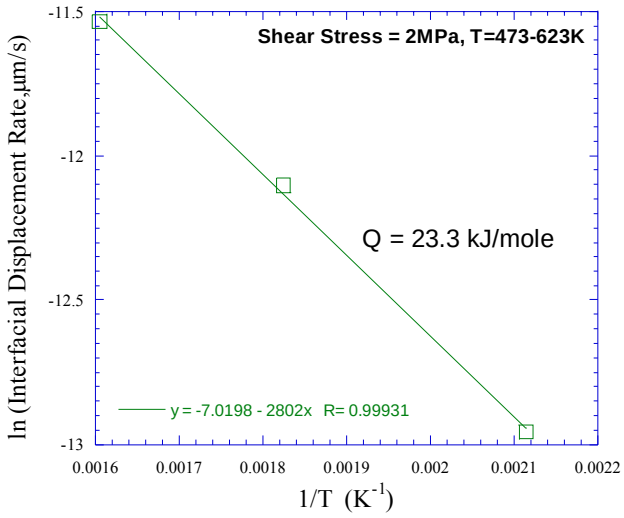

Figure 23. Temperature Dependence of Interfacial Displacement Rate with Apparent Activation Energy of ~23.3kJ/mole

THIS PAGE INTENTIONALLY LEFT BLANK

V. CONCLUSIONS

An experimental methodology to analyze the kinetics of interfacial creep at the Al thin film/silicon substrate interface was refined and tested. The proposed sample geometry consisted of an Al thin film deposited on a polished Si substrate, via vacuum evaporation, with another polished Si being diffusion-bonded to the top surface of the Al film. The resultant Si/Al thin film/Si sandwich was then etched and grooved to produce shear stresses at the Al/Si interfaces when the sample is loaded edge-wise in compression. The details of the sample preparation technique and the apparatus used to load the sample for conducting the creep test are reported.

By measuring the interface displacement rates at varying temperatures and stresses, the kinetic parameters for interface sliding were experimentally determined. The experiments conducted showed that Al-Si interfaces undergo diffusionally accommodated sliding under shear stresses at high temperatures. A threshold stress was recorded, apparently due to the presence of some unintended compression at the interface. But more testing is needed to properly understand the effects of the change in geometry and loading conditions of the test specimen.

The activation energy was found to be lower than that documented by research reported earlier [10]. Potential reasons for this are discussed. The potential for sliding along both interfaces must be investigated further. Future modeling studies to better understand the impact of the complicated sample and loading geometries used in the test are suggested.

THIS PAGE INTENTIONALLY LEFT BLANK

LIST OF REFERENCES

1. Funn, J. V., and Dutta, I., "Creep Behavior of Interfaces in Fiber Reinforced Metal-Matrix Composites", Acta Mater., 47, pp. 149-164, 1999

2. Peterson, K. A., Dutta, I, and Chen, M. W., Scripta Mater., 2002, in press.

3. Peterson, K. A., Dutta, I., and Chen, M. W., "Diffusionally Accommodated Interfacial Sliding in Metal-Silicon Systems", Acta Mater., 2003, in press

4. Peterson, K. A., Park, C. and Dutta, I., in Silicon Materials-Processing, Characterization and Reliability, Proc. 2002 MRS Spring Mtg., in press.

5. Dutta, I., Chen M.W., Peterson, K., and Shultz, T., "Plastic Deformation and Interfacial Sliding in Al and Cu Thin Film: Si Substrate Systems Due to Thermal Cycling", Journal of Electronic Materials., Vol. 30, No. 12, pp.1537-1548, 2001.

6. Park, C., Dutta, I., Peterson, K.A., and Vella, J., "Deformation and Interfacial Sliding in Back-End Interconnect Structures in Microelectronic Devices", Journal of Electronic Materials, Vol. 32, No.10, pp.1059-1071, 2003.

7. Zhmurkin, D. V., Gross, T. S., and Buchwalter, L. P., "Interfacial Sliding in Cu/Ta/Polyimide High Density Interconnects as a Result of Thermal Cycling", J. Electronic. Mater., 26, p. 791, 1997.

8. Zhmurkin,D. V., Gross, T. S. and Buchwalter, L.,P., "Interfacial Sliding in Cu/Ta/Polyimide High Density Interconnects as a Result of Thermal Cycling", in 'Creep and Stress Relaxation in Miniature Structures and Components', H. D. Merchant, ed., TMS-AIME, 1997, pp. 255-270

9. Hu, C. K., Luther, B., Kaufman, F. B., Hummel, J., Thin Solid Films, 262, p. 84, 1995

10. Peterson, K. A., "Measurements and Observations of Interfacial Creep in engineering Systems", Dissertation, Naval Postgraduate School, September 2002

11. Thouless, M. D., Gupta, J. and Harper, J. M. E., "Stress Development and Relaxation in Copper Films During Thermal Cycling", J. Mater Res., 8, pp. 1845-1852, 1993.

12. Shen, Y. L. and Suresh, S., "Steady-State Creep of Metal-Ceramic Multilayered Materials", Acta Mater., 44, pp. 1337-1348, 1996.

13. Chen, M. W. and Dutta, I., Appl. Phys. Let., 77, pp. 4298, 2000.

14. Suhir, E., “Approximate Evaluation of the Elastic Interfacial Stresses in Thin Films with Application to High-Tc Superconducting Ceramics”, Int. J. Solids Structures, 27, pp. 1025-1034, 1991.

15. Suhir, E., “Stresses in Bi-Metal Thermostats”, J. Appl. Mech. 53, pp. 657-660, 1987.

16. Suresh, S., Giannakopoulos, A. E. and Ollson, M. J., Mech Phys. Solids, 42, p. 979, 1994.

17. Lambropoulos, J. C. and Wan, S. M., “Stress Concentration Along Interfaces of Elastic-Plastic Thin Films”, Mater. Sci. Eng., A107, pp. 169-175, 1989.

18. Dutta, I., Mutra, S., West, A. D., “Some Effects of Thermal Residual Stresses onthe Strain Response of Graphite-Aluminum Composites During Thermal Cycling”, in Residual Stresses in Composites, E. V. Barrera and I. Dutta, eds., TMS-AIME, Warrendale, Pennsylvania, pp. 273-292, 1993.

19. Dutta, I., “Role of Interfacial and Matrix Creep During Thermal Cycling of Continuous Fiber Reinforced Metal-Matrix Composites”, Acta Mater., Vol. 48, pp. 1055-1074, 2000.

20. Yoda, S. Kurihara, N. Wakashima, K. and Umekawa, S., “Thermal Cycling Induced Deformation of Fibrous Composites with Particular Reference to the Tungsten-Copper System”, Metall. Trans, 9A, pp. 1229-1236, 1978.

21. Mitra, S., Dutta, I. and Hansen, R. C., “Thermal Cycling Studies of Cross-Plied P100 Graphite Fiber Reinforced 6061 Aluminum Composite Laminate”, J. Mater. Sci., 26, p. 6223, 1991.

22. Furness, J. A. G. and Clyne, T. W., “Application of Scanning Laser Extensometry to Explore Thermal Cycling creep of Metal Matrix Composites”, Mater. Sci. Engng., A141, pp. 199-207, 1991.

23. Cox, B. N., “Interfacial Sliding Near Free Surface in a Fibrous or Layered Composite During Thermal Cycling”, Acta Metall. Mater., 38, pp. 2411-2424, 1990.

24. Nagarajan, R., Dutta, I., Funn, J. V. and Esmele, M., “Role of Interfacial Sliding on the Longitudinal Creep Response of Continuous Fiber Reinforced Metal-Matrix Composites”, Mater, Sci. Engng., A259, pp. 237-252, 1999.

25. Dutta, I., “Role of Interfacial and Matrix Creep During Theraml Cycling of Continuous Fiber Reinforced Metal-Matrix Composites”, Acta Mater., Vol. 48, pp. 1055-1074, 2000.

26. Artz, E., Ashby, M. F. and Verall, R. A., Acta Metall., "Interface Controlled Diffusional Creep", 31, pp. 1977-1989, 1983.

27. Ashby, M.F., "On Interface-Reaction of Nabarro-Herring Creep and Sintering", Scripta Metall., Vol. 3, pp. 837-842, 1969.

28. Stang, R. G. and Barrett, C. R., "Newtonian Viscous Creep in Fe-3%Si", Scripta Metall. 7, p. 233, 1973.

29. Sautter, F. K. and Chen, E. S., Proc. Bolton Landing Conf. on Oxide Dispersion Strengthening, Gordon & Breach, New York, p. 495, 1969.

30. Ignat, M. and Bonnet, R., "Role of Phase Boundaries in the Hot Deformation in Tension of Al-$CuAl_2$ Single Eutectic Grains – A Deformation Model", Acta Metall., 31, pp. 1991-2001, 1983.

31. Gupta, D., Vieregge, K. and Gust, W., "Interface Diffusion in Eutectic Pb-Sn Solder", Acta Mater., 47, pp. 5-12, 1999.

32. Vala, J., Svoboda, J. Kozak, V. and Cadek, J., "Modeling Discontinuous Metal Matrix Composite Behavior under Creep Conditions: Effect of Interface Diffusional Matter Transport and Interface Sliding", Scripta Metall. Mater., 30, pp. 1201-1206, 1994.

33. Iyengar, N. and Curtin, W. A., "Time Dependent Failure in Fiber-Reinforced Composites be Matrix and Interface Shear Creep", Acta Mater., 45, pp. 3419-3429, 1997

34. Meyer, D. W., Cooper, R. F. and Plesha, M. E., "High Temperature Creep and the Interfacial Mechanical Response of Ceramic Matrix Composites", Acta Metall. Mater., 41, pp. 3157-3170, 1993.

35. Mori, T., Tanaka, K., Nakasone, Y., Huang, J. and Taya, M., "Creep of a Metal Matrix Composite with or without Diffusion and Sliding on Matrix/Reinforcement Interfaces", Key Engng Mater., Vols. 137-131, pp. 1145-1152, 1997.

36. Jobin, V. C., Raj, R. and Phoenix, S. L., "Rate Effects in Metal-Ceramic Interface Sliding from the Periodic Film Cracking Technique", Acta Metall. Mater., 40, pp. 2269-2280, 1992.

37. Raj, R. and Ashby, M.F., "On Grain Boundary Sliding and Diffusional Creep", Metall. Trans., 2, pp. 1113-1127, 1971.

38. Humphreys, F. J., Miller, W. S., Djazeb, M. R., Mater. Sci. Tech., Vol. 6, p. 1157, 1990.

39. Humphreys, F. J., Kalu, P. N., Acta Metall., Vol. 38, p. 917, 1990.
40. Humphreys, F. J., Acta Mater., Vol. 45, p. 5031, 1997.

41. Mishra, R. S. and Mukherjee, A. K., "On Superplasticity in Silicon Carbide Reinforced Aluminum Composites", Scripta. Metall. Mater., 25, pp. 271-275, 1991.

42. Mishra, R. S., Bieler, T. R. and Mukherjee, A. K., "Superplasticity in Powder Metallurgy Aluminum Alloys and Composites", Acta Metall. Mater., 43, pp. 877-891, 1995.

43. Mishra, R. S., Bieler, T. R. and Mukherjee, A. K., "Mechanism of High Strain Rate Superplasticity in Aluminum Alloy Composites", Acta Mater., 45, pp. 561-568, 1997.

44. Rosler, J. and Evans, A. G., "Effects on Reinforcement Size on the Creep Strength of Intermetallic Matrix Composites", Mater. Sci. Engng., A153, pp. 438-443, 1992.

45. Goto, S. and Mclean, M., "Role of Interfaces in Creep of Fiber-Reinforced Metal-Matrix Composites:I. Continuous Fibers", ACta Metall. Mater., 39, pp. 153-164, 1991.

46. Bullock, E., Mclean, M. and Miles, D. E., "Creep Behavior of Ni-Ni_3Al-Cr_3C_2 Eutectic Composite", Acta Metall., 25, pp. 333-344, 1977.

47. Kim, K. T. and McMeeking, R. M., "Power Law Creep with Interface Slip and Diffusion in Composite Material", Mech. Mater., 20. pp. 153-164, 1995.

48. Nimmagadda, P. B. R. and Sofronis, P., " Creep Strength of Fiber and Particulate Composite Materials: The Effect of Interface Slip and Diffusion", Mech. Mater., 23, pp. 1-19, 1996.

49. Sofronis, P. and McMeeking, R. M., "Effects of Interface Diffusion and Slip on the Creep Resistance of Particulate Composite Materials", Mech. Mater., 18, pp. 55-68, 1992.

50. Peterson, K. A., Dutta, I., and Chen, M.W. "Processing and Characterization of Diffusion Bonded Al-Si Interfaces" Journal of Materials Processing Technology, 2003, in press.

51. Yan, G., Chan, P.C.H, Hsing, I., Sharma, R.K., Sin, J.K.O., and Wang, Y., "An Improved TMAH Si-Etching Solution Without Attacking Exposed Aluminum", Sensors and Actuators, A89, pp. 135-141, 2001.

52. Tabata, Osamu, “pH-Controlled TMAH Etchants for Silicon Micromachining”, Sensors and Actuators, A53, pp. 335-339, 1996.

53. Tabata, O., Asahi, R., Funabashi, H., Shimaoka, K., and Sugiyama, S., “Anisotropic Etching of Silicon in TMAH Solutions”, Sensors and Actuators, A34, pp. 51-57, 1992.

54. ASM Metals Handbook, 9th Ed, Metals Park, Ohio, p. 65, 1986.

55. Thornell, M. E., "Sample Fabrication and Experimental Design for Studying Interfacial Creep at Thin Film/Silicon Interfaces ", Master’s Thesis, Naval Postgraduate School, December 2003.

56. Thong, J.T.L., Choil, W.K., and Chong, C.W., “TMAH Etching of Silicon and the Interaction of Etching Parameters”, Sensors and Actuators, A63, pp. 243-249, 1997.

57. Frost, H.J., and Ashby, M.F., “Deformation Mechanisms Maps , The Plasticity and Creep of Metals and Ceramics ,” Pergamon Press, New York, 1982.

THIS PAGE INTENTIONALLY LEFT BLANK

INITIAL DISTRIBUTION LIST

1. Defense Technical Information Center
   Ft. Belvoir, Virginia

2. Dudley Knox Library
   Naval Postgraduate School
   Monterey, California